

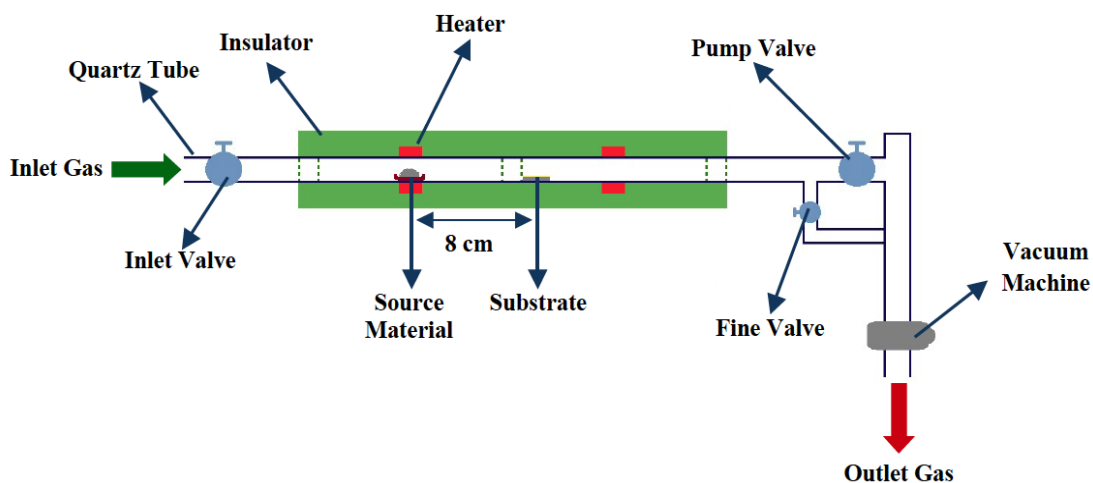
Supplementary Information

Single-crystalline CdTe nanowire field effect transistor as a nanowire-based photodetector

*Mehrdad Shaygan, Keivan Davami, Nazli Kheirabi, Changi Ki Baek
Gianaurelio Cuniberti, M. Meyyappan, and Jeong-Soo Lee*

Nanowire growth

A schematic view of the furnace used for the CdTe nanowire synthesis by the vapor-liquid-solid (VLS) technique is shown in figure S1. In this system, the carrier gas transports the source material vapors from upstream to downstream in the quartz tube. The CdTe powder (Alfa company, 99.99%), 0.03g for all samples, was placed in a high-purity alumina crucible located at the source position of the quartz tube. A silicon wafer substrate was thermally oxidized to obtain a silicon oxide layer (150 nm) and then 1 nm gold layer was deposited on the substrate by electron beam evaporator. The position of the silicon substrate in the growth region was determined by comparing the obtained results for 6 substrates, placed along the entire area of the synthesis region. There is a temperature gradient in the growth region in the quartz tube and therefore we selected the best position where we obtained the highest CdTe growth density. Prior to beginning the heating process, the air in the system was purged by flushing with nitrogen inside the quartz tube. Then the gases inside the tube were removed using a vacuum pump at $\sim 10^{-3}$ Torr. This process was repeated three times to ensure that oxygen was completely eliminated. Then the system was heated at a rate of 20 °C/min to the set temperatures under constant Ar and H₂ flow rates of 10 and 5 standard cubic centimeter per minute (scm). The system was cooled down to room temperature under vacuum conditions after a 60 minute synthesis period when a dark gray coating on the substrate was observed.



Effect of process variables on CdTe nanowire growth

A lower temperature for sublimation than the melting point of the material is one of the main benefits of vapor phase growth route, which results in lower defects and higher crystallographic orientation in the grown crystal [1]. By selecting temperatures higher than 700 °C in the source region, the probability of growing nanowires is more than other types of nanostructures such as nanosaws and nanobelts, while the source temperature must still be lower than the melting point of the raw materials. Davami et al. [2] succeeded in growing various ZnTe nanostructures including nanowires, tapered nanowires, multi-prolonged thin nanowires, and nanoribbons by altering the source temperature. In the first part of our experiments, various temperatures were tried to find the sublimation temperature of CdTe. We succeeded in sublimation of CdTe at lower temperatures and lower pressures compared to the report by Greenberg et al. [3]. Various temperatures from 500 to 700 °C were selected for optimization of the source temperature, while the substrate temperature and the chamber pressure were set at 450 °C and 180 Torr, respectively with a carrier gas mixture of Ar and H₂ (10 and 5 sccm respectively). SEM images of the samples sublimated at 680, 670, 660, and 650 °C are shown in figure S2. At 680 °C, the powders sublimated and deposited on the substrate but the density of grown nanowires was small in 1 μm² area. By decreasing the source temperature to 670 °C, the number of nanostructures increased, although the density of nanowires was still sparse. As the source temperature was lowered to 660 °C, the nanowire coverage on the substrate was high in comparison with 650 °C. The diameter of the nanowires is in the range of 100-150 nm and their lengths are less than 2 μm. The number of tapered nanowires at this temperature is very high, which could be due to the high temperature in the substrate area [4]. Tapered nanowires might be seen at higher temperatures in the substrate region due to the evaporation of gold nanoparticles existing in the tip of nanowires or migration of gold atoms from the tip to the base of the nanowires [2]. As seen in figure S2d, no nanowires grew at 650 °C, which could be attributed to the fact that the temperature gradient between the source and substrate was not high enough and the vapors condensed before reaching the substrate.

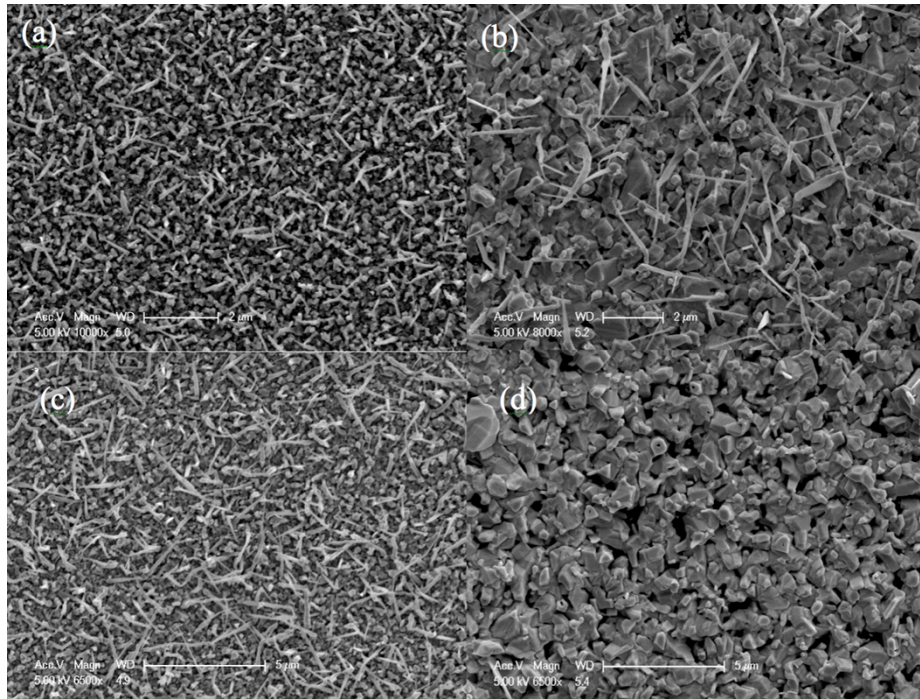


Figure S2: SEM images of the grown structures at different source temperatures of (a) 680 °C, (b) 670 °C, (c) 660 °C, and (d) 650 °C

The substrate temperature is a crucial variable in VLS growth that controls the sample surface kinetics while the source temperature determines the precursor impinging rate on the substrate [5]. Selecting a lower temperature for synthesis, while minimizing unwanted effects including catalyst migration, also broadens the range of feasible substrates [6]. In order to investigate the effect of substrate temperature on CdTe nanowire growth, a wide range of temperatures from 410 to 500 °C were chosen. Figure S3 shows CdTe nanowires grown at different substrate temperatures while the source temperature was set at 660 °C and the chamber pressure at 180 Torr for a carrier gas mixture of Ar and H₂ with flow rates of 10 and 5 sccm, respectively. As shown in figure S3a, at 460 °C, CdTe particles are formed with dimensions less than 5 μm. Lowering the substrate temperature to 450 °C starts nanowire growth but also produces nanoribbons with tapered tips. The number of grown nanowires is not comparable with that of nanoribbons and the diameter of the nanowires is typically less than 100 nm with a length up to 6 μm. Raising the growth temperature at a fixed source temperature can result in a transition from nanowires to nanoribbons [7]. Kar et al. [8] succeeded to grow CdS nanowires and nanoribbons by varying the substrate temperature, where higher temperatures led to the growth of nanoribbons. On the other hand, high temperatures in the substrate area lead to a decrease in the length of the nanowires and an increase in their diameter [9]. In other materials such as ZnTe and CdS, the formation of nanowires and nanoribbons takes place in a wide range of source temperatures [2, 8],

while the range for CdTe here is rather narrow.

In summary, CdTe nanowire growth is very sensitive to the synthesis temperature. A substrate temperature of 440 °C results in large quantity of CdTe nanowires with diameters in the range of 35 to 150 nm and lengths up to 8 μm. Interestingly, the growth rate of nanowire is suppressed by decreasing the synthesis temperature to 430 °C and a great amount of nanoparticles are detected.

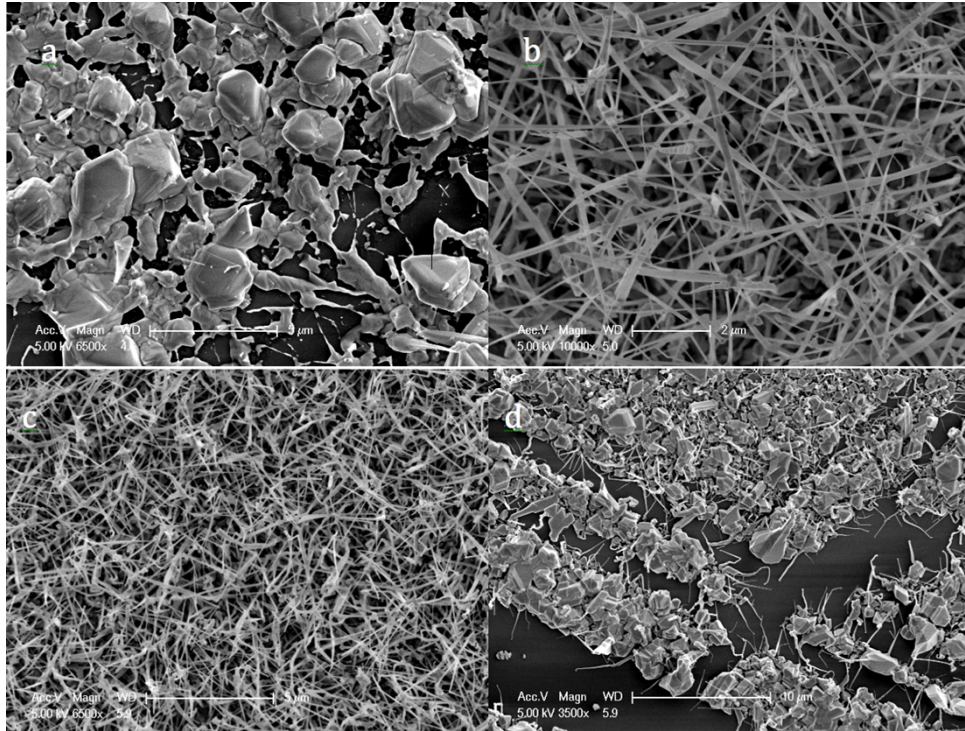


Figure S3: SEM images of the grown structures at different substrate temperatures of (a) 460°C, (b) 450 °C, (c) 440 °C, and (d) 430 °C

Though the effect of reactor pressure is not normally investigated, it can be expected to influence the growth characteristics; for example high pressure and high temperature guarantee the growth of CdSe nanowires with desirable morphology [10]. Romain et al. [11] reported a pressure-dependent growth rate for growing Si nanowires. We conducted growth studies under various pressures of 210, 180, 150, and 130 Torr at the optimized temperature of 660 °C for the source and 440 °C for the substrate (figure S4). At 210 Torr, the number of nanoparticles is more dramatic than that of nanowires. Increased amount of nanowires can be seen at 180 Torr. The reduction in pressure causes an increase in nanowire length as also noticed by Inoue et al. [4] for GaN nanowires due to variation in surface diffusion length. On the other hand, lowering the pressure to 150 Torr increased the number of nanoribbons significantly. Reducing the pressure to 130 Torr led to mostly nanoparticles with a few nanowires in 10 μm².

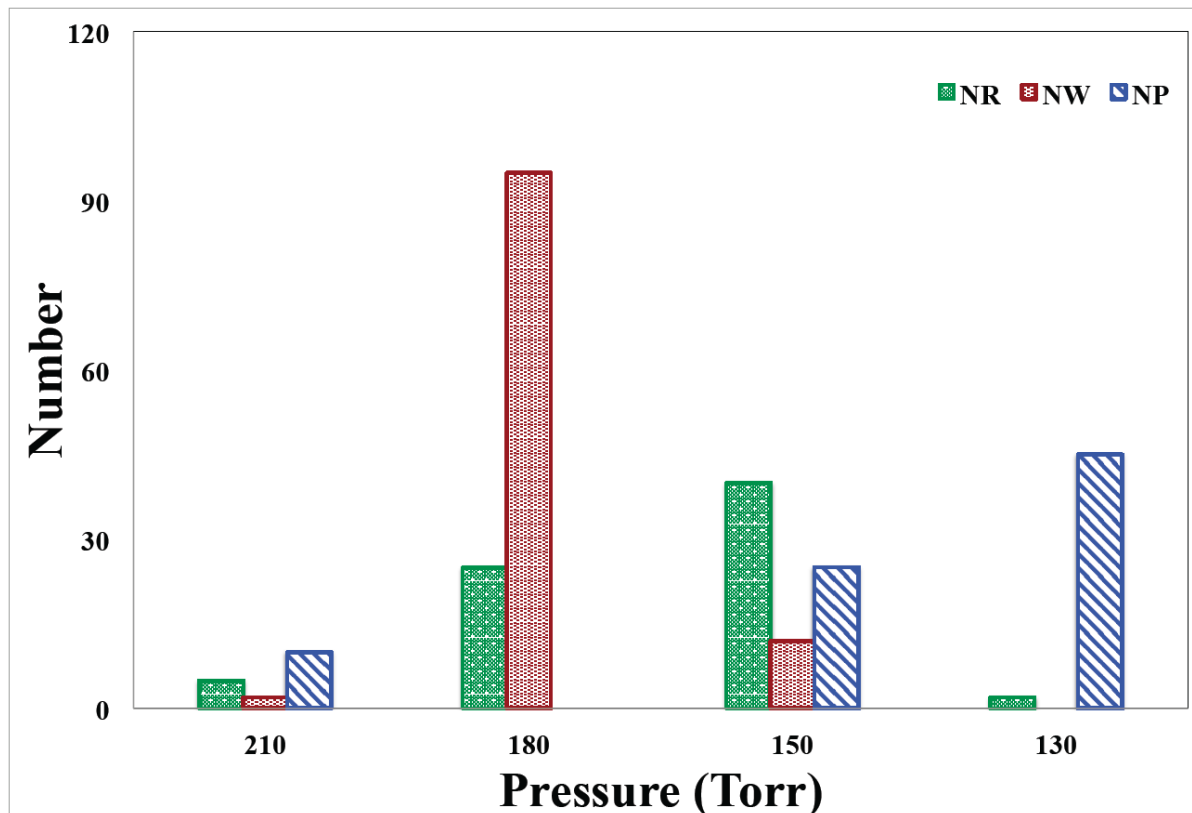


Figure S4: Distribution of grown nanostructures (nanowires, nanoribbons and nanoparticles) at different pressures of (a) 210 Torr, (b) 180 Torr, (c) 150 Torr, and (d) 130 Torr

XRD characterization of CdTe nanowires

The XRD spectra of samples confirmed the high crystalline structure of CdTe since sharp peaks were observed (as shown in figure S5). There are two-crystal structures for CdTe nanostructures, namely zincblende and wurtzite. The total energies of these two structures are equal, neglecting slight differences. One of these two structures could be stabilized through controlled growth conditions. These structures are very similar and the zincblende and wurtzite structures belong to the cubic system hexagonal space group, but the main difference is generated only by their third-nearest-neighbor atomic arrangement. Zincblende structure is well investigated but wurtzite structure of CdTe is not well understood and CdTe is stable in the zincblende structure [12]. The crystal structure of our CdTe NWs was determined as zincblende since three main peaks can be indexed as (111), (220), and (311) peaks in the XRD patterns corresponding to $2\theta=23.78^\circ$, 39.36° , 46.46° , respectively, according to JCPDS card no. 15-0770. A peak in $2\theta = 27.56^\circ$ is attributed to (101) peak SiO_2 (JCPDS card no. 79-1912), which is from the substrate material. CdTe nanowires preferentially grow in [111] direction since the relative (111) diffraction peak intensity for CdTe nanowires is higher than that of JCPDS card no.15-0770. Other planes in the XRD spectra including (400), (331), (422), and (551) diffracted from the following degrees as 56.74° , 62.38° , 71.18° , and 76.03° , respectively. Potlog et al. [13]

noticed the same peaks for CdTe thin films crystallized in the zincblend structure as we see here; they revealed that the same planes were seen in 2θ equal to 23.7° , 39.2° , 46.4° , 56.6° , 62.3° , 71.1° , and 76.18° . The estimation of lattice constants (a) of the nanowire for preferentially oriented (111) reflection from the XRD pattern is calculated as 0.6481 nm, while it is 0.6490 nm for CdTe thin film [13] and 0.6280 nm for CdTe nanowire [14].

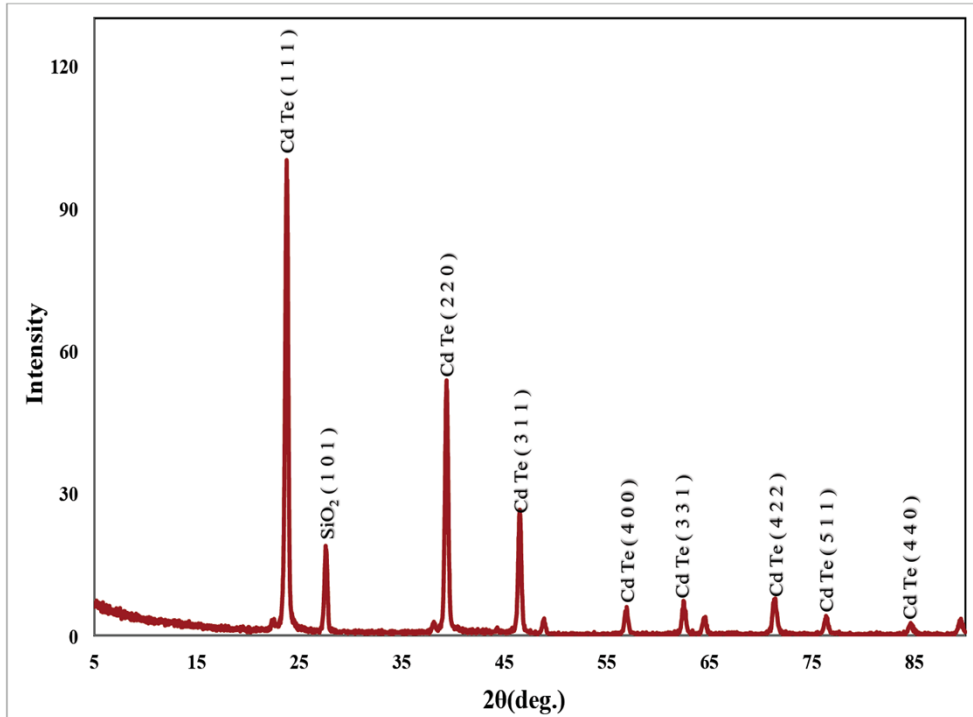


Figure S5. XRD pattern of the grown CdTe nanowire

Raman characterization of CdTe nanowires

Raman spectroscopy confirmed the composition of our CdTe 1D nanostructures as shown in Figure S6. The peak at 138 cm^{-1} is assigned to the transverse optical (TO) mode and the peak at 159 cm^{-1} is attributed to the longitudinal optical (LO) mode of CdTe. As expected, the TO mode intensity is smaller than that of the LO mode [15]. There is a peak at 325 cm^{-1} , which is the second-order CdTe LO phonon scattering. These peaks are similar to the ones reported for CdTe powders by Park et al. [16] at 140 and 160 cm^{-1} for the TO and LO modes. In figure S6, there are two more relatively weak peaks at 62 cm^{-1} and 108.5 cm^{-1} . The first one can be attributed to the disorder-activated transverse or longitudinal acoustic modes [16]. The peak at 108.5 cm^{-1} can be assigned to the TeO_2 Raman peak, which was previously reported for CdTe thin films [17]. In the same report the peaks assigned to the TO mode and LO mode for CdTe were observed at 140 and 160 cm^{-1} respectively. Raman spectroscopy is capable of detecting the atomic disorder in the structure and no effects due to impurities were observed here.

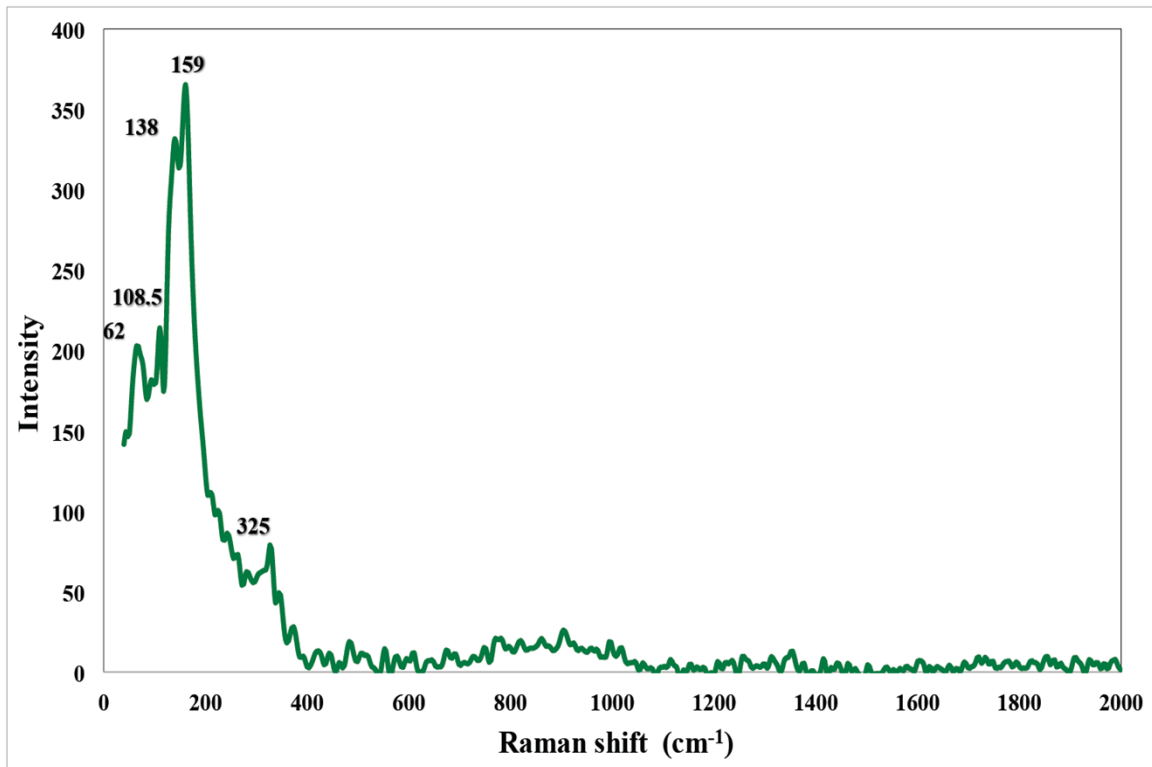


Figure S6. Raman spectroscopy analysis of the CdTe nanowire

References

- [1] J. H. Greenberg, *J. Cryst. Growth*, **197**, 406-412, 1999.
- [2] K. Davami, D. Kang, J. S. Lee, M. Meyyappan, *Chem. Phys. Lett.*, **504**, 62-66, 2011.
- [3] J. H. Greenberg, V. N. Guskov, V. B. Lazarev, *Mat. Res. Bull.*, **27**, 997-1001, 1992
- [4] Y. Inoue, A. Tajima, A. Ishida, H. Mimura, *Phys. Stat. Sol. C.*, **5**, 3001, 2008.
- [5] M. A. Herman, H. Sitter, *Molecular Beam Epitaxy*, Springer, ISBN 3-540-19075-9, 1989.
- [6] A. Coli, A. Fasoli, P. Beecher, P. Servati, S. Pisana, Y. Fu, A. J. Flewitt, W. I. Milne, J. Robertson, C. Ducati, S. S. Franceschi, S. Hofmann, A. C. Ferrari, *J. Appl. Phys.*, **102**, 034302, 2007.
- [7] R. Venugopal, P. I. Lin, C. -C. Liu, Y. T. Chen, *J. Am. Chem. Soc.*, **127**, 11262-11268, 2005.
- [8] S. Kar, S. Chaudhuri, *J. Phys. Chem. B.*, **110**, 4542-4547, 2006.
- [9] O. Yang, J. Sha, L. Wang, Z. Su, X. Ma, J. Wang, D. Yang, *J. Mater. Sci.*, **41**, 3547-3552, 2006.
- [10] C. Ma, Z. L. Wang, *Adv. Mater.*, **17**, 1-6, 2005.
- [11] L. L. Romain, C. Mouchet, C. Cayron, E. Rouviere, J. P. Simonato, *J. Nanopart. Res.*, **10**, 1287-1291, 2008.
- [12] S. -H. Wei, S. B. Zhang, *Phys. Rev. B.*, **62**, 6944-6947, 2000.
- [13] T. Potlog, N. Spalatu, N. Maticiu, J. Hiie, V. Valdna, V. Mikli, A. Mere, *Phys. Stat. Soli. A*, **209**, 272-276, 2012.
- [14] K. Davami, H. M. Ghassemi, X. Sun, R.S. Yassar, J. S. Lee, M. Meyyappan, *Nanotechnology*, **22**, 435204, 2011.
- [15] S. L. Lopez, S. J. Sandoval, O. J. Sandoval, E. C. Perez, M. M. Lira, *J. Vac. Sci. Technol. A.*, **17**, 1958-1962, 1999.
- [16] W. Park, H. S. Kim, S. Y. Jang, J. Park, S. Y. Bae, M. Jung, H. Lee, J. Kim, *J. Mater. Chem.*, **18**, 875-880, 2008.
- [17] J. H. Ruelas, M. L. Lopez, O. Z. Angel, *Jpn. J. Appl. Phys.*, **39**, 1701-1705, 2000.